

Dynamical mechanism of the liquid film motor

Zhong-Qiang Liu,¹ Ying-Jun Li,^{1,*} Guang-Cai Zhang,² and Su-Rong Jiang³

¹*State Key Laboratory for GeoMechanics and Deep Underground Engineering, SMCE, China University of Mining and Technology, Beijing 100083, China*

²*National Key Laboratory of Computational Physics, Institute of Applied Physics and Computational Mathematics, Beijing 100088, China*

³*Qindao College, Qingdao Technological University, Qingdao 266106, China*

(Received 21 July 2010; revised manuscript received 15 November 2010; published 8 February 2011)

The paper presents a simple dynamical model to systemically explain the rotation mechanism of the liquid film motor reported by experiments. The field-induced-plasticity effect of the liquid film is introduced into our model, in which the liquid film in crossed electric fields is considered as a Bingham plastic fluid with equivalent electric dipole moment. Several analytic results involving the torque of rotation, the scaling relation of the threshold fields, and the dynamics equation of a square film and its solution are obtained. We find that the rotation of the liquid film motor originates from the continuous competition between the destruction and the reestablishment of the polarization equilibrium maintained by the external electric field, which is free from the boundary effects. Most experimental phenomena observed in direct current electric fields are interpreted well.

DOI: [10.1103/PhysRevE.83.026303](https://doi.org/10.1103/PhysRevE.83.026303)

PACS number(s): 68.15.+e, 47.65.Gx, 83.60.La, 77.22.Ej

I. INTRODUCTION

Recently much attention has been focused on the effects of the electric fields on the liquid films. On the one hand, macroscopic thin films are important in physics, biophysics, and engineering [1]. On the other hand, the effects of the electric fields on the liquid films not only bring about many unexpected phenomena but also exhibit potential application prospects in microfluidic systems to mix or phase separate liquids or particles in microscale systems [2].

The electric fields can produce electrohydrodynamical flows in free suspended films, which are made of either certain liquid crystals [3–7] or common polar liquids [8–11]. Recently, Amjadi *et al.* [11] reported an interesting experimental device, the so-called liquid film motor, as the direction and the speed of its rotation can be controlled via manipulating the direction and the strength of the applied electric fields. Meanwhile, experiments bring about several thought-provoking questions: What causes the liquid film motor to rotate? Why are the points near the center rotating faster than those away from it? Why do the threshold fields obey a simple scaling relation? For the first question, Amjadi *et al.* [11] denied the possibility of generating such a flow by the edge effects or ionization of the water molecules, and proposed a heuristic explanation based on the changing of the orientation of water molecular dipoles due to a strong electric field. To our knowledge, two papers have attempted to give a reasonable physical explanation for the first two questions [12,13]. However, they did not give the answers to the third question. Moreover, for further experiments, few theoretical guidance is currently available.

In this paper, a simple physical model is introduced to systemically explain the dynamical mechanism of the liquid film motor [11]. The purpose is to discover the physical origin behind the fluid phenomena occurring in the crossed electric fields, with the hope of developing an essential understanding for these counterintuitive phenomena. All questions that we

have mentioned are systemically answered in this paper. We find that the rotation of the liquid film in crossed electric fields originates from the continuous competition between the destruction and the reestablishment of the polarization equilibrium maintained by the external electric field, which is free from the boundary effects of the liquid film.

The remainder of this paper is organized as follows. We will introduce the model and dynamical mechanism in Sec. II. The scaling relation of the threshold fields is analytically given in Sec. III. Section IV is devoted to deducing the dynamics equation of a square film and its solution. Finally, in Sec. V some concluding remarks and discussions are made.

II. MODEL AND DYNAMICAL MECHANISM

In this section, we first give some evidence in favor of our assumption: the liquid film exhibits plastic behavior in an applied electric field and then produces a qualitative picture of the dynamical mechanism responsible for the liquid film motor. Finally, the active torque driving the rotation of the liquid film motor is presented.

Quantum field theory produces a picture of liquid water as a mixture of two phases [14–16], which are a low-density coherent phase made up of extended regions, the so-called coherence domains (CDs) where all water molecules oscillate in phase between two configurations, and a high-density noncoherent phase made up of independent molecules trapped in the interstices among the CDs (0.1 μm). In normal water, CDs are not necessarily correlated among each other. However, the coherence among CDs can be induced by an externally applied polarization field [17,18]. Recently two articles in favor of the proposed theory appeared [19,20]. In addition, based on this theory, many “anomalous” phenomena of the water observed in experiments can be explained, such as “Neowater” [21], “EZ Water” [22–24], and “Floating Water Bridge” [17,25,26].

In the case of the floating water bridge the external electric field can align the CDs to form superdomains [25–28]. Recently, a two-dimensional neutron-scattering study

*lyj@aphy.iphy.ac.cn

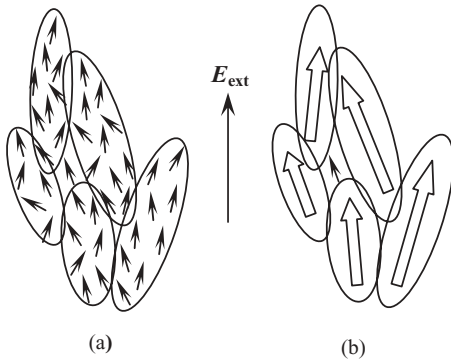


FIG. 1. (a) The polarization equilibrium maintained by the external electric field. Each ellipse denotes a CD. Arrows “ \uparrow ” represent the dipolar orientations of the polar molecules. (b) The equivalent of (a). Arrows “ \uparrow ” denote the orientations and values of the equivalent dipole moments of CDs.

indicated a low-level long-range molecular ordering within a D_2O bridge [29]. Moreover, Widom *et al.* [30] pointed out that in a polar liquid acting as a ferrofluid, the electric-field-induced tension responsible for holding up the water bridge arises out of long ordered chains of low-entropy aligned coherent dipolar domains. The case of the floating water bridge is similar to that of the liquid film in an external electric field. It is conceivable that within the liquid film located in an external electric field **there must be long ordered chains parallel to the field, which are responsible for the plasticity of the film, just as the particle chains are responsible for the plastic behavior of electrorheological fluids** [31].

The thin water film is almost completely made up of CDs [32]. When it is located in an external electric field \vec{E}_{ext} produced by a large parallel-plate capacitor, it will reach a polarization equilibrium, and **a permanent polarization develops in each CD** [14] [see Fig. 1(a)]. As the liquid film is very thin (hundreds of nanometers or less), the motions of CDs are restricted in a quasi-two-dimensional space. For the same reason, the orientational preference of equivalent dipole moment of each CD is almost **completely parallel to the external electric field \vec{E}_{ext}** [see Fig. 1(b)], since **the disruptive role of thermal collisions gets neutralized by the external electric field and the surface tension**. As a result, the equivalent dipole moment per unit volume is so large that it may **bring about a powerful torque** in a high steady electric field \vec{E}_{cur} , which drives the liquid film to move. However, experimental results show that rotation can not be observed in relatively thick film (or a bulk of liquids) [11]. Among the possible explanations of this phenomenon, the most plausible is that the equivalent dipole moment per unit volume is too small to start the rotation, since the orientational preference of the independent molecules exposed to the disruption of the thermal collisions become disordered in the thick film or bulk water. In other words, the necessary preconditions for the rotation of the liquid film depend on the thickness of the film. Therefore, if not otherwise stated, the liquid film discussed in this paper is so thin that it may rotate in crossed electric fields.

As we have mentioned, if the applied crossed steady electric field \vec{E}_{cur} is large enough, it will destroy the polarization

equilibrium maintained by \vec{E}_{ext} . In fact, as a fully coherent water, the strong correlated motions of CDs constitute the macroscopical motion of the liquid film, since it is impossible to touch a molecule without affecting all the others. Almost at the same time \vec{E}_{ext} will rapidly reestablish the polarization equilibrium kept by itself. (\vec{E}_{ext} should play a dominant role in the polarization of the liquid film since \vec{E}_{ext} exists in the whole space between two plates of a large parallel-plate capacitor, while \vec{E}_{cur} , which causes the electric current, exists only within the liquid film.) In this way, the continuous destruction effect of the steady electric field \vec{E}_{cur} on the polarization equilibrium maintained by \vec{E}_{ext} creates the rotating flow of the liquid film. That is to say, the motion of the liquid film results from the continuous competition between the destruction and the reestablishment of the polarization equilibrium maintained by the external electric field.

From the macroscopic viewpoint a compartment of the liquid film may be realized as an unaltered equivalent electric dipole in the whole process. Based on the picture we have described, the thin liquid film in the crossed electric fields is considered as a Bingham plastic fluid with an equivalent electric dipole moment.

The dynamical mechanism of the liquid film motor is considered from the viewpoint of the action of the mechanical torques on the liquid film, which was first introduced by Grosu and Bologna [13]. Without loss of generality, the thin liquid film (l_1, l_2, h) is artificially partitioned into several rectangular compartments [see Fig. 2(a)]. A compartment (a, b, h) [e.g., a gray compartment in Fig. 2(a)] with fixed-plane free surfaces ($z = 0, -h$) in Cartesian coordinates (x, y, z) is investigated [see Fig. 2(b)]. For convenience, the direction of the electric current density \vec{J}_{cur} (or \vec{E}_{cur}) is along the y direction. θ denotes the angle between the external electric field \vec{E}_{ext} and \vec{J}_{cur} .

First, let us consider the case under the following conditions: $\theta = 90^\circ$, $\vec{E}_{\text{ext}} \neq 0$, and $\vec{J}_{\text{cur}} = 0$. The external electric field induces the opposite polarization charges in the fluid near the interface boundaries of the studied compartment [see Fig. 2(b)]. As we have mentioned, compartment (a, b, h) may be considered as an equivalent electric dipole parallel to the external electric field \vec{E}_{ext} . The corresponding dipole moment is expressed as

$$\vec{P} = \frac{\epsilon_0(\epsilon_r - 1)V}{\epsilon_r} \vec{E}_{\text{ext}}, \quad (1)$$

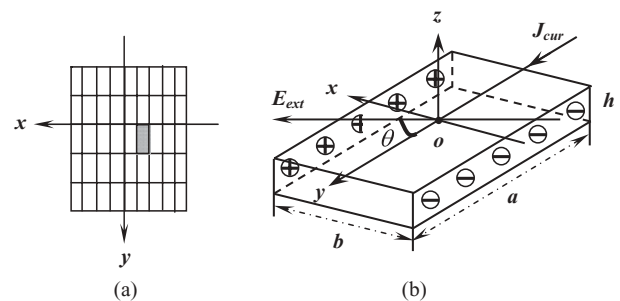


FIG. 2. (a) A planform of the thin liquid film. (b) A sketch of a rectangular compartment of the thin liquid film in the crossed electric fields.

where ε_0 , ε_r , and $V = abh$ denote the dielectric constant of vacuum, the relative dielectric constant of the liquid, and the volume of the studied compartment, respectively.

Subsequently, turning on the electrolysis current ($\vec{J}_{\text{cur}} \neq 0$), the equivalent dipole moment \vec{P} will be subject to the steady electric field \vec{E}_{cur} . The torque \vec{M}_{cur} exerted on \vec{P} may be defined as

$$\vec{M}_{\text{cur}} = \vec{P} \times \vec{E}_{\text{cur}}. \quad (2)$$

Inserting Eq. (1) into Eq. (2), we obtain the active torque which drives the rotation of the liquid film:

$$\vec{M}_{\text{cur}} = \frac{\varepsilon_0(\varepsilon_r - 1)}{\varepsilon_r} E_{\text{ext}} E_{\text{cur}} V \sin \theta \vec{e}_z. \quad (3)$$

This result is also suitable for the compartment of arbitrary shape by extrapolation.

Equation (2) reveals that the direction of the torque \vec{M}_{cur} obeys a simple right-hand rule, which is in the form of $\vec{E}_{\text{ext}} \times \vec{E}_{\text{cur}}$ (or $\vec{E}_{\text{ext}} \times \vec{J}_{\text{cur}}$). This result coincides with the rotation direction of the induced vortices observed in the laboratory [11]. From Eq. (3) it is easy to understand the experimental phenomenon that the rotation velocity monotonically drops to zero as the angle θ between \vec{E}_{ext} and \vec{E}_{cur} decreases from 90° to 0° . However, our further investigation predicts that film stops rotating when θ is small enough but not zero. One can obtain such a prediction from the driving source of the liquid film motor given in Sec. IV.

III. SCALING RELATION OF THE THRESHOLD FIELDS

In this section, considering the field-induced-plasticity effect of the thin film of polar liquid, we derive the scaling law of the threshold fields.

For simple shearing flow $u = u(y)$, the constitutive relation for a Bingham plastic fluid is expressed as [33,34]

$$\frac{\partial u}{\partial y} = \begin{cases} 0, & (\tau < \tau_0) \\ (\tau - \tau_0)/\mu, & (\tau \geq \tau_0), \end{cases} \quad (4)$$

where τ_0 is the so-called yield stress and μ represents the plastic viscosity. That is to say, the liquid film does not show its fluid behavior until the shear stress is larger than the yield stress. Otherwise it behaves as a rigid body at low stress.

To start the rotation of the liquid film, the active torque \vec{M}_{cur} exerted on a CD (or a superdomain) must be larger than the maximum static resistance torque arising from the yield stress. It is also convenient to investigate a compartment (a, b, h) . In Cartesian coordinates (x, y, z) , considering the symmetry of the maximum static resistances (see Fig. 3), one may obtain the resultant torque of the maximum static resistance, which is expressed as

$$\vec{M}_f = -2\tau_0 V \vec{e}_z, \quad (5)$$

where $V = abh$, the volume of the studied compartment, and the numerical factor 2 comes from two couples arising from the yield stress. This result is also suitable for a CD (or a superdomain) of arbitrary shape by extrapolation.

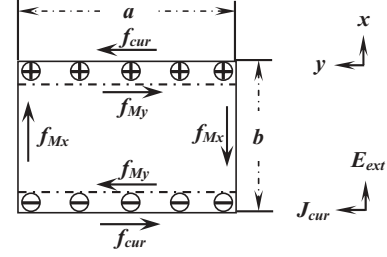


FIG. 3. The free-body force diagram for a compartment (a, b, h) . f_{cur} represents a couple resulting from the interactions between the equivalent dipole moment and the steady electric field. f_{Mx} and f_{My} denote two couples arising from the yield stress.

If the resultant torque exerted on the studied CD is defined as

$$\vec{M}_r = \vec{M}_{\text{cur}} + \vec{M}_f, \quad (6)$$

letting $\vec{M}_r = 0$ and using Eqs. (3), (5), and (6), we have

$$E_{\text{ext}} E_{\text{cur}} \sin \theta = \frac{2\tau_0 \varepsilon_r}{\varepsilon_0(\varepsilon_r - 1)}, \quad (7)$$

which is the scaling relation of the threshold fields. By using the relation between \vec{E}_{cur} and the electrolysis voltage U_{cur} ,

$$U_{\text{cur}} = E_{\text{cur}} l_2, \quad (8)$$

Eq. (7) may be rewritten as

$$E_{\text{ext}} U_{\text{cur}} \sin \theta = \frac{2\tau_0 \varepsilon_r l_2}{\varepsilon_0(\varepsilon_r - 1)}. \quad (9)$$

On the one hand, Eq. (7) shows that the threshold of the fields is independent of electrical conductivity, viscosity, and/or density of the liquid. This prediction coincides with the experimental results that show that the thresholds of the fields are in the same order of magnitude for all the polar liquids with different electrical conductivity, viscosity, and/or density. Although ε_r are on a different order of magnitude for the liquids used in experiments (e.g., water, aniline, anisole, chlorobenzene, and diethyleoxalate) [11], $\varepsilon_r/(\varepsilon_r - 1)$ in Eq. (7) are on the same order of magnitude $O(1)$. Comparison between the experimental and the theoretical results implies that the yield stresses of different liquid films are on the same order of magnitude. Namely, different polar liquids may form a similar ordered structure in an external polarization field. This prediction is partly confirmed by the experimental findings of the group led by G. H. Pollack [24], who found that different polar liquids (e.g., water, methanol, ethanol, isopropanol, and acetic acid) show similar near-surface exclusion zones, due to the polarization field produced by the wall. Obviously, more experiments are called for in order to clearly identify whether this prediction is correct.

On the other hand, Eq. (7) can give an especially good fit of experimental results (see Fig. 4). Setting $\varepsilon_r = 80$ and $l_2 = 3.1 \times 10^{-2}$ m, by fitting the experimental results to Eq. (9), the transform of Eq. (7), we obtain $\tau_0 = 6.77, 7.26$, and $7.75 (\times 10^{-5} \text{ Pa})$. Contrasting Fig. 4 in this paper with Fig. 2 in Ref. [11], we find an interesting phenomenon: the larger volume a fraction of glycerin is, the smaller the yield stress of the water film is. In our opinion, there are two possible reasons.

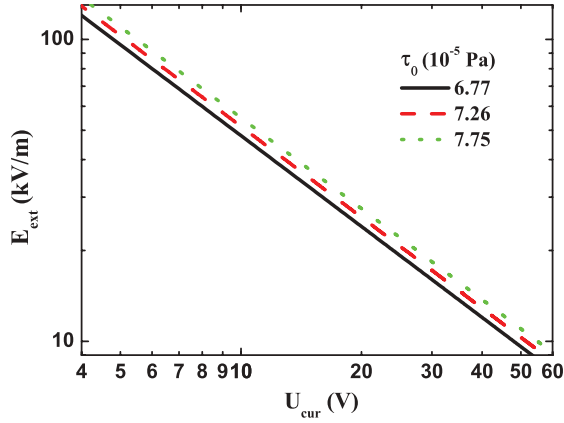


FIG. 4. (Color online) The plot of the electric field versus the electric voltage at the rotating threshold for the solutions with different yield stresses τ_0 ($\times 10^{-5}$ Pa). $\tau_0 = 6.77$ (solid line), $\tau_0 = 7.26$ (dashed line), and $\tau_0 = 7.75$ (dotted line).

One is that, if the thicknesses of the films with different volume fractions of glycerin are the same in experiments, the perturbations of glycerin weaken the coherence among CDs within the water film, further reducing the value of the yield stress of it. Another possible reason is that the larger a volume fraction of glycerin is, the thinner the water film used in the experiments is, and the smaller the yield stress of it is.

IV. DYNAMICS EQUATION AND ITS SOLUTION

In this section, the dynamics equation for a square liquid film (l, l, h) is deduced from the rotational form of Newton's second law. This method is completely different from those that directly start from the Navier-Stokes equations [12,13].

The film is assumed to be thin enough ($h \ll l$) and the surface forces large enough that **the effects of the thickness of the film and the gravity on the film rotation can be ignored**. The present analysis is inspired by the stable ring structure of the rotating square liquid film. We divide the liquid film into a series of concentric cylindrical rings, all of which obey the rotational form of Newton's second law:

$$\vec{M}_r = J \vec{\beta}, \quad (10)$$

where \vec{M}_r denotes the resultant torque exerted on a ring liquid film of radius r and radius $r + dr$, and J and $\vec{\beta}$ are the moment of inertia and the angular acceleration of it, respectively.

In a cylindrical coordinate systems (r, θ, z), one may easily obtain the moment of inertia of the ring liquid film

$$J = \rho r^2 dV, \quad (11)$$

where ρ is liquid density and $dV = 2\pi r h dr$ denotes the volume of the ring liquid film. The angular acceleration of it may be expressed as

$$\vec{\beta} = \omega_t \vec{e}_z = \frac{u_t}{r} \vec{e}_z, \quad (12)$$

where ω_t and u_t , respectively, denote the first partial derivatives of the angular velocity ω and the linear velocity u with respect to time t .

The rest of this work is to deduce the resultant torque exerted on the ring liquid film. Of course, we can directly derive it from the free-body force diagram for the ring liquid film. However, for convenience, we deduce it from the partial derivative of the resultant moment \vec{M}_{rd} exerted on a disc liquid film of radius r with respect to r , which originates from two sources, i.e.,

$$\vec{M}_{rd} = \vec{M}_{curd} + \vec{M}_{Bd}, \quad (13)$$

where \vec{M}_{curd} results from the interactions between the equivalent dipole moment \vec{P} and the steady electric field \vec{E}_{cur} , and \vec{M}_{Bd} derives from the viscosity force. In addition, it can be proved that the contribution to the resultant torque from the hydrodynamics pressure vanishes by considering the periodicity of the pressure over the angle θ .

Using Eq. (3), one can obtain

$$\vec{M}_{curd} = \frac{\epsilon_0(\epsilon_r - 1)}{\epsilon_r} E_{ext} E_{cur} \pi r^2 h \sin \theta \vec{e}_z. \quad (14)$$

From Eq. (4), in cylindrical coordinates, the viscous force exerted on the disc liquid film of radius r is expressed as

$$\vec{f}_{Bd} = \left[\tau_0 - \mu \left(u_r - \frac{u}{r} \right) \right] 2\pi r h (-\vec{e}_\theta), \quad (15)$$

where u_r denotes the first partial derivative of u with respect to r . Its corresponding torque has the following form:

$$\vec{M}_{Bd} = \left[-\tau_0 + \mu \left(u_r - \frac{u}{r} \right) \right] 2\pi r^2 h \vec{e}_z. \quad (16)$$

Inserting Eqs. (14) and (16) into Eq. (13), we have

$$\vec{M}_{rd} = \left(\Delta + 2\mu u_r - \frac{2\mu u}{r} \right) \pi r^2 h \vec{e}_z, \quad (17)$$

where

$$\Delta = \epsilon_0(1 - 1/\epsilon_r) E_{ext} E_{cur} \sin \theta - 2\tau_0. \quad (18)$$

By taking a partial derivative of Eq. (17) with respect to r , we obtain the resultant torque exerted on the ring liquid film of radius r and radius $r + dr$:

$$\vec{M}_r = \left(\mu r u_{rr} + \mu u_r - \frac{\mu u}{r} + \Delta \right) dV \vec{e}_z, \quad (19)$$

where u_{rr} denotes the second partial derivative of u with respect to r .

Inserting Eqs. (11), (12), and (19) into Eq. (10), we finally obtain the dynamics equation of the square liquid film:

$$u_t = \frac{\mu}{\rho r^2} (r^2 u_{rr} + r u_r - u) + \frac{\Delta}{\rho r}, \quad (0 < r < R, t > 0). \quad (20)$$

Equation (20) indicates that Δ is the driving source of the rotation of the liquid film motor. The liquid film motor can work with direct current electric fields only if $\Delta > 0$. Thus, given $\Delta = 0$, one can obtain the scaling relation of the threshold fields Eq. (7) from Eq. (18) at once.

There are two boundary conditions and an initial condition for Eq. (20): the disappearance of the linear velocity at $r = 0$ and $r = R$, and the liquid film is static at $t = 0$, i.e.,

$$u(r, t)|_{r=0} = 0, \quad u(r, t)|_{r=R} = 0. \quad (21)$$

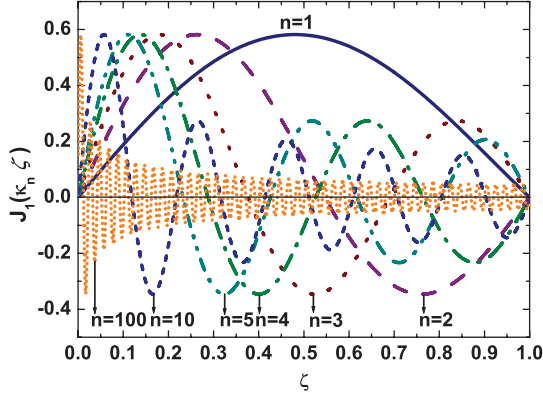


FIG. 5. (Color online) Several modes of the linear velocity $J_1(\kappa_n \zeta)$ for different κ_n ($k_1 = 3.832$, $k_2 = 7.016$, $k_3 = 10.173$, $k_4 = 13.324$, $k_5 = 16.471$, $k_{10} = 32.190$, $k_{100} = 314.943$), where $\zeta = r/R$, which is a dimensionless variable from 0 to 1.

and

$$u(r, t)|_{t=0} = 0. \quad (22)$$

The solution of this problem can be obtained by separation of variables. It is expressed as

$$u(r, t) = \Delta \sum_{n=1}^{\infty} c_n J_1\left(\frac{\kappa_n r}{R}\right) (1 - e^{-a_n t}), \quad (23)$$

where

$$c_n = \frac{2R}{\mu} \frac{1 - J_0(\kappa_n)}{\kappa_n^3 J_0^2(\kappa_n)}, \quad a_n = \frac{\mu}{\rho} \frac{\kappa_n^2}{R^2}, \quad (24)$$

κ_n denotes the n th zero point of $J_1(Z)$, ordinary Bessel function of order one, and $J_0(Z)$ is an ordinary Bessel function of order zero. The corresponding angular velocity has the following form:

$$\omega(r, t) = \frac{\Delta}{r} \sum_{n=1}^{\infty} c_n J_1\left(\frac{\kappa_n r}{R}\right) (1 - e^{-a_n t}). \quad (25)$$

Physically, the rotation of the liquid film exhibits many spatial modes. Some modes of the linear velocity and the angular velocity for different κ_n are illustrated in Figs. 5 and 6, respectively. It is apparent that these modes show an

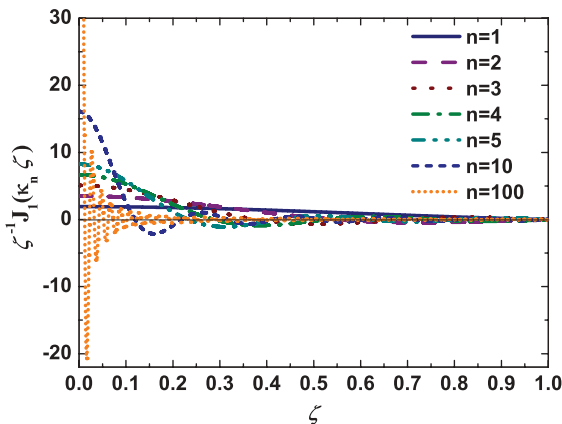


FIG. 6. (Color online) Several modes of the angular velocity $\zeta^{-1} J_1(\kappa_n \zeta)$ for the same parameters as in Fig. 5.

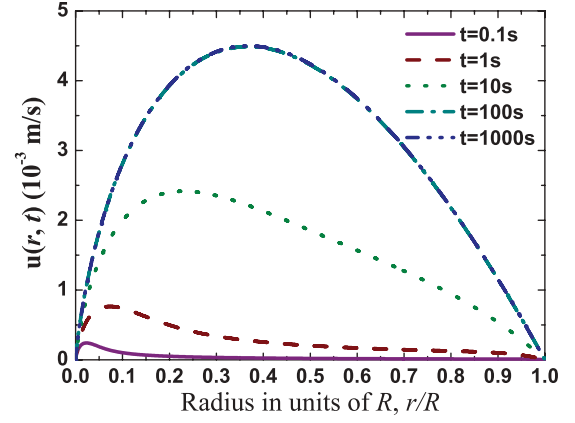


FIG. 7. (Color online) The profiles of the linear velocity for different times: $t = 0.1$ s, 1 s, 10 s, 100 s, 1000 s.

oscillatory decreasing behavior as the radius r increases from 0 to R . Equations (23) and (25) indicate that as time evolves, modes with different κ_n appear in sequence. When time is long enough, all modes constitute the stationary rotation of the liquid film. Under the circumstances, Eqs. (23) and (25) are simplified as

$$u(r, t \rightarrow \infty) = \frac{\Delta}{2\mu} r \ln \frac{R}{r} \quad (26)$$

and

$$\omega(r, t \rightarrow \infty) = \frac{\Delta}{2\mu} \ln \frac{R}{r}. \quad (27)$$

Here Eq. (26) is identical with the result in reference [13].

Using Eqs. (23) and (25), setting $E_{\text{ext}} E_{\text{cur}} \sin \theta = 7.2 \times 10^6$ V²/m, $l = 2R = 3.1 \times 10^{-2}$ m, $\mu = 10^{-3}$ Pa·s and $\tau_0 = 6.77 \times 10^{-5}$ Pa, we plot the profiles of the linear velocity (see Fig. 7) and the angular velocity (see Fig. 8) for different times. Figures 7 and 8 illustrate that the points near the center start to rotate earlier than those away from it. Subsequently the points away from the center gradually start to move. As the rotation radius r increases from zero, the rotation speed increases quickly from zero to a maximum and then decreases slowly to zero as r increases further (see Fig. 7). As time

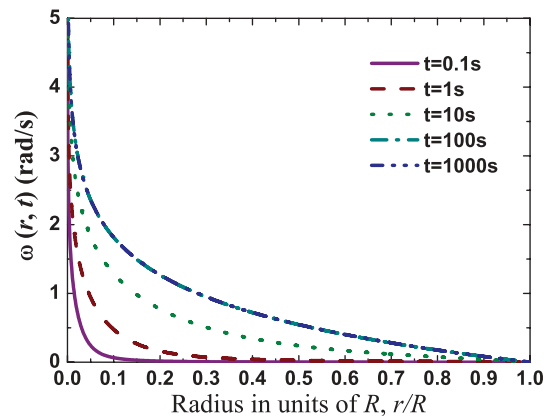


FIG. 8. (Color online) The profiles of the angular velocity for the same parameters as in Fig. 7.

evolves, the location of the maximum of the linear velocity moves away from the center of the film. Finally, the linear velocity has its maximum at

$$r_m = R/e. \quad (28)$$

At a fixed time, the angular velocity decreases as the radius r increases from 0 to R (see Fig. 8). This result is consistent with the experimental one (see Fig. 3 in Ref. [11]).

V. CONCLUSIONS AND DISCUSSIONS

A simple physical model is presented in this paper to systemically explain the dynamical mechanism of the liquid film motor. Considering the liquid film in the crossed electric fields as a Bingham plastic fluid with equivalent electric dipole moment, we successfully explain most of the experimental phenomena observed in direct current electric fields. Several analytical results, such as the torque of rotation, the scaling relation of the threshold fields, and the dynamics equation of a square film and its solution, are obtained. The comparison between our theoretical predictions and the experimental results is presented in detail. We find that the rotation of the liquid film in crossed electric fields originates from the continuous competition between the destruction and the reestablishment of the polarization equilibrium maintained by the external electric field, which is free from the boundary effects. Several interesting phenomena are predicted in the paper. For example, **the polar liquid films of arbitrary shape may rotate in the crossed electric fields**. For square liquid film, the rotation speed has its maximum at $r = R/e$ when the rotation of the film is stable.

Our model indicates why the addition of an amount of salt to water almost cannot affect the speed of the rotation. Although the addition of an amount of salt to water may increase the liquid electrical conductivity by a few orders of magnitudes, **the speed of rotation [Eq. (23)] is free of the liquid electrical conductivity** and is mainly dependent on μ , ρ , R , and Δ [$\Delta = \varepsilon_0(1 - 1/\varepsilon_r)E_{\text{ext}}E_{\text{cur}}\sin\theta - 2\tau_0$]. Addition of an amount of salt to water may change the density ρ and the relative dielectric constant ε_r of the liquid. However, they could not noticeably affect the speed of rotation.

Experiments show that one cannot observe any induced rotation in films of nonpolar liquids [11]. Why? Perhaps the films of nonpolar liquids would also show a plastic behavior in an external electric field. Recently, Rai *et al.* [35] demonstrated that an external electric field can induce a covalent-like bond between polar and nonpolar molecular species. However, in contrast to the polar liquids, **without the relatively strong orientational polarization, the equivalent dipole moment of the molecule groups in the nonpolar liquids is too small to break this plasticity**. Naturally, one cannot observe the induced rotation in films of nonpolar liquids.

ACKNOWLEDGMENTS

This work is supported by National Basic Research Program of China under Grant No. 2007CB815105, and National Natural Science Foundation of China under Grant No. 11074300. ZQL would like to acknowledge many fruitful discussions with Li-Feng Wang, Yan-Biao Gan, and Hong-Wei Li.

-
- [1] P. Nelson, *Biological Physics: Energy, Information, Life* (W. H. Freeman, New York, 2003).
 - [2] T. M. Squires and S. R. Quake, *Rev. Mod. Phys.* **77**, 977 (2005).
 - [3] A. A. Sonin, *Freely Suspended Liquid Crystalline Films* (John Wiley & Sons, New York, 1998).
 - [4] S. Faetti, L. Fronzoni, and P. A. Rolla, *J. Chem. Phys.* **79**, 5054 (1983).
 - [5] S. Faetti, L. Fronzoni, and P. A. Rolla, *J. Chem. Phys.* **79**, 1427 (1983).
 - [6] S. W. Morris, J. R. de Bruyn, and A. D. May, *Phys. Rev. Lett.* **65**, 2378 (1990).
 - [7] Z. A. Daya, S. W. Morris, and J. R. de Bruyn, *Phys. Rev. E* **55**, 2682 (1997).
 - [8] A. Ramos, H. Morgan, N. G. Green, and A. Castellanos, *J. Phys. D* **31**, 2338 (1998).
 - [9] R. Shirsavar *et al.*, e-print [arXiv:condmat/0605029](https://arxiv.org/abs/condmat/0605029).
 - [10] A. Amjadi, R. Shirsavar, N. Hamedani Radja, and M. R. Ejtehadi, e-print [arXiv:0805.0490v2](https://arxiv.org/abs/0805.0490v2).
 - [11] A. Amjadi, R. Shirsavar, N. Hamedani Radja, and M. R. Ejtehadi, *Microfluid Nanofluid* **6**, 711 (2009).
 - [12] E. V. Shiryaeva, V. A. Vladimirov, and M. Yu. Zhukov, *Phys. Rev. E* **80**, 041603 (2009).
 - [13] F. P. Grosu and M. K. Bologa, *Surface Engineer. Appl. Electrochem.* **46**, 43 (2010).
 - [14] E. Del Giudice, G. Preparata, and G. Vitiello, *Phys. Rev. Lett.* **61**, 1085 (1988).
 - [15] E. Del Giudice and G. Vitiello, *Phys. Rev. A* **74**, 022105 (2006).
 - [16] R. Arani, I. Bono, E. Del Giudice, and G. Preparata, *Int. J. Mod. Phys. B* **9**, 1813 (1995).
 - [17] E. Del Giudice, E. C. Fuchs, and G. Vitiello, *Water* **2**, 69 (2010).
 - [18] E. C. Fuchs, *Water (MDPI)* **2**, 381 (2010).
 - [19] C. Huang *et al.*, *Proc. Natl. Acad. Sci. USA* **106**, 15214 (2009).
 - [20] C. A. Yinnon and T. A. Yinnon, *Mod. Phys. Lett. B* **23**, 1959 (2009).
 - [21] Y. Katsir, L. Miller, Y. Aharonov, and E. Ben Jacob, *J. Electrochem. Soc.* **154**, D249 (2007).
 - [22] J. C. Henniker, *Rev. Mod. Phys.* **21**, 322 (1949).
 - [23] J. M. Zheng *et al.*, *Adv. Colloid Interface Sci.* **127**, 19 (2006).
 - [24] B. Chai and G. H. Pollack, *J. Phys. Chem. B* **114**, 5371 (2010).
 - [25] E. C. Fuchs *et al.*, *J. Phys. D* **40**, 6112 (2007).
 - [26] J. Woisetschlager, K. Gatterer, and E. C. Fuchs, *Exp. Fluids* **48**, 121 (2010).
 - [27] E. C. Fuchs *et al.*, *J. Phys. D* **41**, 185502 (2008).

- [28] E. C. Fuchs *et al.*, *J. Phys. D* **42**, 065502 (2009).
- [29] E. C. Fuchs, P. Baroni, B. Bitschnau, and L. Noirez, *J. Phys. D* **43**, 105502 (2010).
- [30] A. Widom, J. Swain, J. Silverberg, S. Sivasubramanian, and Y. N. Srivastava, *Phys. Rev. E* **80**, 016301 (2009).
- [31] M. V. Gandhi and B. S. Thompson, *Smart Materials and Structures* (Chapman & Hall, London, 1992).
- [32] E. Del Giudice and G. Vitiello, e-print [arXiv:1009.6014v1](https://arxiv.org/abs/1009.6014v1).
- [33] E. C. Bingham, U. S. Bureau of Standards Bulletin **13**, 309 (1916).
- [34] J. F. Steffe, *Rheological Methods in Food Process Engineering* (Freeman, East Lansing, MI, 1996).
- [35] D. Rai, A. D. Kulkarni, S. P. Gejji, and R. K. Pathak, *Theor. Chem. Acc.* **123**, 501 (2009).